World Journal of Engineering Research
Print ISSN: 2959-9865
Online ISSN: 2959-9873
DOI: https://doi.org/10.61784/wjer3110

IMOGWO-BASED STRUCTURAL OPTIMIZATION OF A DUAL-DRIVE FEED SYSTEM UNDER MULTI-FORCE COUPLING

FangYong Xu*, JunShuo Cui, ZhuoYue Li, RunJia Yu, ZhenKai Luan
School of Mechanical and Electrical Engineering, Shandong Jianzhu University, Jinan 250101, China.
**Corresponding Author: FangYong Xu*

Abstract: This study presents an RSM- and IMOGWO-based structural optimization method for a dual-drive feed system worktable under multi-force coupling conditions. A finite element model is established, and three structural depths are selected as design variables to minimize mass and maximum coupling stress while maximizing the first-order natural frequency. A response surface surrogate model is constructed from orthogonal experiments, and the improved MOGWO is used for multi-objective optimization. The optimized design reduces mass by 6.58% and maximum coupling stress by 1.60%, while increasing the first-order natural frequency by 0.065%. Finite element validation verifies the reliability of the proposed method.
Keywords: IMOGWO algorithm; Response surface model; Multi-objective optimization; Dual-drive feed system; Multi-force coupling

1 INTRODUCTION

The dual-drive feed system of high-end CNC machine tools is critical to high-speed, high-precision machining. Under multi-force coupling conditions, the worktable must balance lightweight design, high stiffness, and strong vibration resistance, making multi-objective optimization a key engineering challenge. Response Surface Methodology (RSM) efficiently constructs surrogate models from limited samples, thereby reducing the cost of repeated finite element analysis. RSM has been widely applied in mechanical structure optimization, with Hernandez-Vazquez et al. investigating stiffness characteristics of machine tool joints and Ma et al. and Li et al. demonstrating its effectiveness in multi-factor and lightweight design optimization [1-3]. The Multi-Objective Grey Wolf Optimizer (MOGWO) has attracted considerable attention for its simple structure, strong global search capability, and effective Pareto set maintenance, as initially proposed by Mirjalili et al. [4], with subsequent improvements including Boltzmann-selection-based MOGWO [5], PSO-GWO hybrid optimization [6], and applications in microgrid operation and gas fractionation [7,8].
For dual-drive feed systems, Huang et al. applied NSGA-II to worktable optimization [9]; however, traditional algorithms still suffer from limited convergence accuracy, uneven Pareto distribution, and weak local search capability in high-dimensional, strongly constrained, and multimodal problems. To address these issues, this study develops a multi-objective structural optimization method under multi-force coupling conditions by combining a SolidWorks-based finite element model, a second-order RSM surrogate model, and an improved MOGWO. The optimized design reduces mass by 6.58% and maximum coupling stress by 1.60%, while increasing the first-order natural frequency by 0.065%.

2 THREE-DIMENSIONAL MODELING, FINITE ELEMENT ANALYSIS, AND OPTIMIZATION MODELING

2.1 Three-Dimensional Modeling and Finite Element Preprocessing

The worktable, as the core moving component of the dual-drive feed system, directly affects lightweight performance, stiffness, and vibration resistance. During 3D modeling in SolidWorks, structural features of mature machine tools, including the WCH63, DMG MORI NHX 6300, Mazak HCN-4000, and Shenyang i5H series, were referenced. The final model preserves key weight-reduction structures and critical fit relationships, as shown in Figure 1.

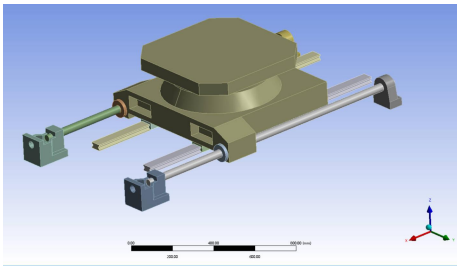

Figure 1 3D Assembly Model of the Dual-Drive Feed System

The 3D worktable model is imported into ANSYS Workbench 2022 R1 for multi-force coupling finite element analysis under gravity and standard cutting loads. Minor fillets and chamfers are removed to improve mesh quality and computational efficiency. The worktable is assigned HT200 gray cast iron, while the ball screw, bearings, nut, and sliders use GCr15 bearing steel. Bonded contact is defined between the ball screw and nut, and frictional contact with a coefficient of 0.08 is applied between sliders and guide rails. Automatic meshing with local refinement is performed mainly using Solid187 tetrahedral elements, resulting in 264,171 nodes and 537,443 elements. Mesh quality indicators confirm that the model is reliable for subsequent static and modal analyses. Figure 2 presents the worktable mesh and preliminary results.

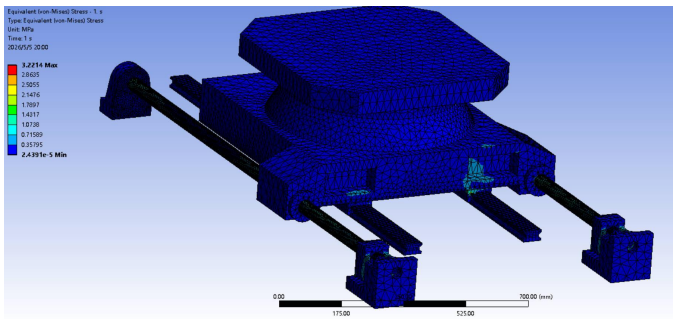

Figure 2 System Meshing and Preliminary Simulation Results

2.2 Optimization Workflow and Determination of Design Variables

The multi-objective optimization procedure consists of 3D modeling, finite element initialization, definition of design variables and objectives, construction of a response surface surrogate model, and IMOGWO-based Pareto optimization, followed by verification of the optimal scheme. The depths of the end-face rectangular hole, weight-reduction cavity, and inner rectangular hole (Figure 3, Table 1) are chosen as key design variables because they define the main weight-reduction regions and strongly affect mass distribution and structural stiffness. Although greater depths reduce redundant material, inertia, and energy consumption, they may also induce stress concentration or excessive deformation. Coordinated optimization is therefore adopted to balance mass, stiffness, and dynamic performance while improving the first-order natural frequency to suppress chatter.

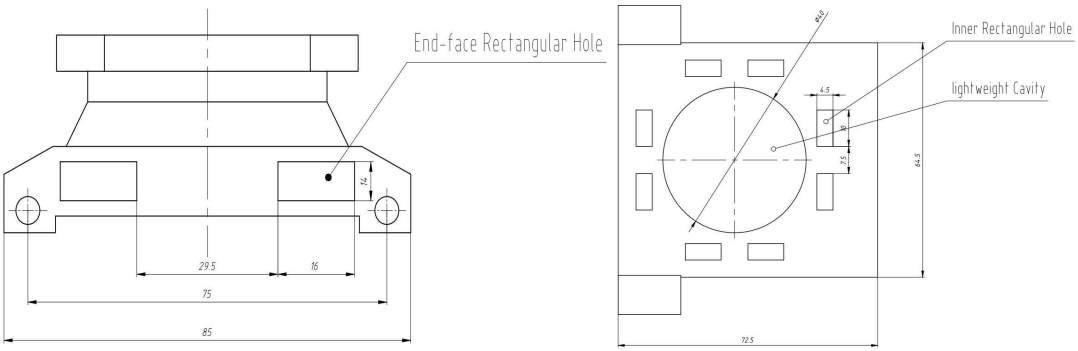

Figure 3 Schematic Diagram of Rectangular Holes and Weight-reduction Cavities

Table 1 Comparison of Power Load Forecasting of 403 Line

Size parameters to be optimized	Original data	Value range
Depth of weight-reduction cavity	50	25~75
Depth of inner rectangular hole	50	25~75
Depth of end rectangular hole	75	50~100

2.3 Mathematical Model and Orthogonal Experimental Design

Structural optimization formulates engineering design problems as quantitative mathematical models. In this study, a multi-objective model for the dual-drive feed system is established under dimensional and strength constraints to balance lightweight design, dynamic performance, and multi-force coupling performance, as follows:

$$\left.\begin{array}{l} F(x_1,x_2,x_3)=\min\left(m(x),\sigma(x),-f_1(x)\right) \\ m(x)=F_m(x_1,x_2,x_3) \\ \sigma(x)=F_\sigma(x_1,x_2,x_3) \\ f_1(x)=F_f(x_1,x_2,x_3) \end{array}\right\} \quad \left.\begin{array}{c} s.t. \\ 50\text{mm}\leqslant x_1\leqslant 100\text{mm} \\ 25\text{mm}\leqslant x_2\leqslant 75\text{mm} \\ 25\text{mm}\leqslant x_3\leqslant 75\text{mm} \\ \sigma_{\max}\leqslant[\sigma] \end{array}\right\} \tag{1}$$

Where F_m denotes the worktable mass function, F_σ represents the maximum coupling stress function, and F_f denotes the first-order natural frequency function; σ_{max} is the maximum coupling stress, and $[\sigma]$ is the allowable material stress. The independent variables x_1,x_2 and x_3 correspond to the depths of the end-face rectangular hole, weight-reduction cavity, and inner rectangular hole, respectively.The corresponding orthogonal experimental factors and levels are listed in Table 2.

Table 2 Table of Orthogonal Experimental Factors and Levels

Level	Factor		
	Depth of end rectangular hole x_1(mm)	Weight-reduction cavity depth x_2(mm)	Inner rectangular hole depth x_3(mm)
+1	100	75	75
0	75	50	50
-1	50	25	25

Response Surface Methodology is used to map the worktable structural parameters to the multi-force coupling performance objectives. The orthogonal test results are listed in Table 3. Based on these data, Design-Expert 13 constructs second-order polynomial response surface models with linear, quadratic, and interaction terms using the least squares method, as follows.

Table 3 Orthogonal Test Results

Orthogonal test number	Orthogonal test factor			Orthogonal experiment results		
	x_1 (mm)	x_2 (mm)	x_3 (mm)	Workbench mass	Maximum coupling stress	fundamental frequency(Hz)
1	50	25	25	801.528kg	3.2214 MPa	216.97
2	50	25	75	788.568kg	3.2968 MPa	174.53
3	50	75	25	756.289kg	3.2534 MPa	220.28
4	50	75	75	743.329kg	3.1725 MPa	210.76
5	100	25	25	793.464kg	3.9996 MPa	213.99
6	100	25	75	780.504kg	4.0756 MPa	212.47
7	100	75	25	748.255kg	4.0030 MPa	217.18
8	100	75	75	735.265kg	4.0573 MPa	215.74
9	75	25	50	791.016kg	3.4153 MPa	206.50
10	75	75	50	745.777kg	3.5996 MPa	217.84
11	75	50	25	774.876kg	3.5661 MPa	216.89
12	75	50	75	761.916kg	3.6146 MPa	215.45
13	50	50	50	772.428kg	3.2583 MPa	217.98
14	100	50	50	764.364kg	3.9976 MPa	208.04
15	75	50	50	768.396kg	3.4091 MPa	208.07
16	75	50	50	801.528kg	3.2214 MPa	216.97

3 MULTI-OBJECTIVE OPTIMIZATION SOLUTION BASED ON RSM AND IMOGWO ALGORITHM

3.1 Design of the Fitting Functions

Response Surface Methodology is employed to establish the mapping between the structural parameters of the dual-drive feed system worktable and the multi-force coupling performance objectives. Based on the orthogonal experimental data, Design-Expert 13 is used to construct second-order polynomial response surface models with linear, quadratic, and interaction terms by the least squares method, as expressed below.

$$\left.\begin{aligned} F_m(x_1,x_2,x_3) =& 838.69330-0.161515x_1-0.905127x_2 \\ &-0.258807x_3+6.0\times10^{-6}x_1x_2 \\ &-6.0\times10^{-6}x_1x_3-6.0\times10^{-6}x_2x_3 \\ &+2.36620\times10^{-6}x_1^2+3.16620\times10^{-6}x_2^2 \\ &+2.36620\times10^{-6}x_3^2 \\ F_\sigma(x_1,x_2,x_3) =& 3.57262-0.013132x_1+0.002392x_2 \\ &-0.011363x_3+0.000015x_1x_2 \\ &+0.000027x_1x_3-0.000036x_2x_3 \\ &+0.000178x_1^2-0.000015x_2^2 \\ &+0.000118x_3^2 \\ F_f(x_1,x_2,x_3) =& 231.28165-0.051600x_1+0.395560x_2 \\ &-1.29044x_3-0.006616x_1x_2 \\ &+0.009800x_1x_3+0.006600x_2x_3 \end{aligned}\right\} \quad (2)$$

Variance and significance analyses in Design-Expert indicate that all response surface models have very high coefficients of determination and adjusted coefficients of determination. This demonstrates that the fitted polynomials accurately capture the effects of structural parameters under multi-force coupling and can serve as reliable surrogate models for subsequent IMOGWO-based optimization.

3.2 The Classical MOGWO Algorithm

The Grey Wolf Optimizer simulates the encircling, hunting, and attacking behaviors of grey wolves to iteratively search for the optimal solution [1]. In multi-objective optimization, it is extended to the Multi-Objective Grey Wolf Optimizer by incorporating an external archive for non-dominated Pareto solutions and using a grid mechanism with roulette-wheel selection to determine the α、β and δ leaders from the archive, which guide the population update. The position update can be expressed as:

$$X(t+1)=\frac{X_1+X_2+X_3}{3} \quad (3)$$

Where X_1,X_2 *and* X_3 represent the position update components guided by the α、β and δ wolves, respectively.Despite its simple structure and strong global search capability, the classical MOGWO still suffers from poor population quality, imbalanced exploration and exploitation, and premature convergence in complex nonlinear problems. Therefore, an improved MOGWO is proposed to enhance convergence accuracy, population diversity, and local search capability.

3.3 The IMOGWO Algorithm

To satisfy the multi-coupling optimization requirements of the dual-drive feed system, five strategies are proposed to enhance the standard MOGWO, as shown in Figure 4, and the corresponding mathematical models and principles are presented below.

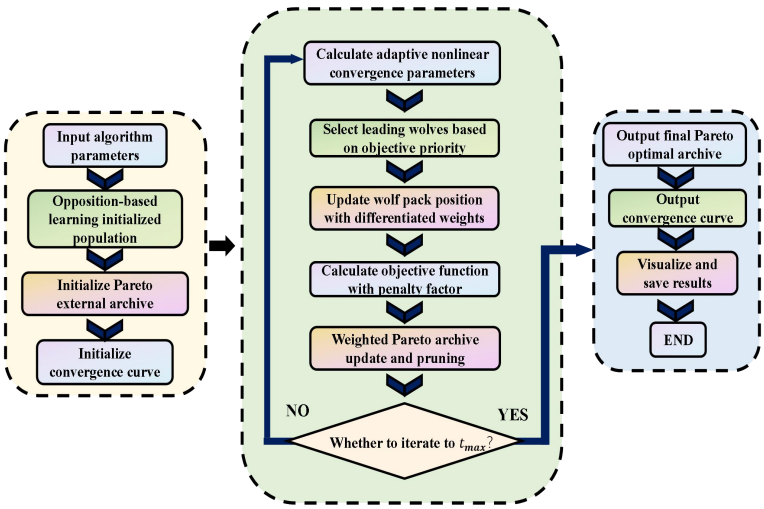

Figure 4 Flowchart of the IMOGWO Algorithm

3.3.1 Opposition-Based Learning (OBL) initialization

To enhance the global search coverage of the initial population, the IMOGWO algorithm, building upon the randomly generated initial original solutions $X_{i,j}$, generates the corresponding opposite solutions $X'_{i,j}$ through an opposition-based learning mechanism:

$$X'_{i,j}=lb_j+ub_j-X_{i,j} \tag{4}$$

Where lb_j and ub_j denote the lower and upper bounds of the j_{th} dimensional variable, respectively. Subsequently, the comprehensive fitness of all solutions is evaluated, and the half of the individuals with the optimal fitness are selected to form the initial population. This effectively mitigates the blindness inherent in traditional random initialization, thereby laying a high-quality initial search foundation for the algorithmic iterations.

3.3.2 Design of the adaptive non-linear convergence parameter

In the standard GWO algorithm, the convergence factor a decreases linearly from 2 to 0, which struggles to adapt to the optimization pace of complex multimodal problems. The IMOGWO algorithm integrates the iteration progress with population diversity (based on the normalized population standard deviation value, Div_{norm} to construct an adaptive non-linear convergence model:

$$a_{base}=2\left[1-\left(\frac{t}{t_{\max}}\right)^2\right] \tag{5}$$

$$a=a_{base}\cdot\left(0.8+0.4\cdot Div_{norm}\right) \tag{6}$$

This model appropriately increases a when the population diversity is high to enhance the global exploration capability; conversely, it decreases a when the diversity is low to accelerate local exploitation. This mechanism achieves a dynamic balance between exploration and exploitation, effectively preventing the algorithm from becoming trapped in local optima.

3.3.3 Differentiated weight updating based on hierarchy

In the standard MOGWO, the guiding weights of the α、β and δ leader wolves are equally distributed (1/3), which fails to reflect the hierarchical differences within the wolf pack and the guiding requirements at different iteration stages. To more authentically reflect the hierarchical system of the wolf pack and accelerate the convergence of the algorithm, the IMOGWO introduces differentiated weight coefficients that change dynamically with the number of iterations:

$$w_\alpha=0.5+0.3\left(\frac{t}{t_{\max}}\right) \tag{7}$$

$$w_\beta=0.3-0.1\left(\frac{t}{t_{\max}}\right) \tag{8}$$

$$w_\delta=1-w_\alpha-w_\beta \tag{9}$$

The corresponding position update formula is improved to $X(t+1)=w_\alpha X_1+w_\beta X_2+w_\delta X_3$. In the later stages of the iteration, the guiding weight of the α wolf (the optimal solution) approaches 0.8. This substantially strengthens the guiding role of the optimal solution and significantly enhances the local convergence accuracy of the algorithm.

3.3.4 Dynamic objective constraints with a penalty factor

To ensure that the optimized solution domain strictly complies with the physical boundaries and design requirements of the machine tool, a quadratic penalty term P is introduced into the objective evaluation functions (response surface equations). When the stress of a candidate solution exceeds the allowable limit [σ] or its frequency falls below the minimum requirement $f_{\min}$, a severe penalty is imposed:

$$P=\lambda_1\cdot\max(0,\sigma-[\sigma])^2+\lambda_2\cdot\max(0,f_{\min}-f_1)^2 \tag{10}$$

$$F_{obj}(X)=f_{RSM}(X)+P \tag{11}$$

Where λ_1,λ_2 denote the extremely large penalty coefficients (set to 1000 in this study). By utilizing the penalty term, the algorithm is forced to circumvent the infeasible region, thereby ensuring that the optimization results strictly satisfy the engineering constraints.

3.3.5 Pareto pruning and leader selection based on objective importance

In the processes of external archive updating and the selection of the α、β and δ leaders, the IMOGWO abandons the single criterion of crowding distance evaluation and constructs a comprehensive fitness evaluation function that integrates the a priori weights of the objectives (stress w_{stress} = 0.5, frequency w_{freq} = 0.3, mass w_{mass} = 0.2):

$$S_{priority}=w_{stress}(1-\hat{\sigma})+w_{freq}(1-\hat{f})+w_{mass}(1-\hat{m}) \tag{12}$$

$$Fitness=0.6\cdot S_{priority}+0.4\cdot D_{crowd} \tag{13}$$

Where $\hat{\sigma}$、$\hat{f}$ and $\hat{m}$ represent the normalized objective values, and D_{crowd} denotes the crowding distance. Using a fusion ratio of 70% priority and 30% crowding distance, this mechanism directs the population toward the preferred region of high vibration resistance and low stress, improving the Pareto front distribution and engineering applicability.

3.4 Solution Results and Verification of the Optimization Model Based on the IMOGWO Algorithm

In this section, IMOGWO is employed to obtain the Pareto optimal solution set for the dual-drive feed system worktable. The algorithm is configured with a population size of 15, 100 iterations, and an archive capacity of 100, and the results are shown in Figure 5. The best overall solution is then selected and validated by finite element simulation.

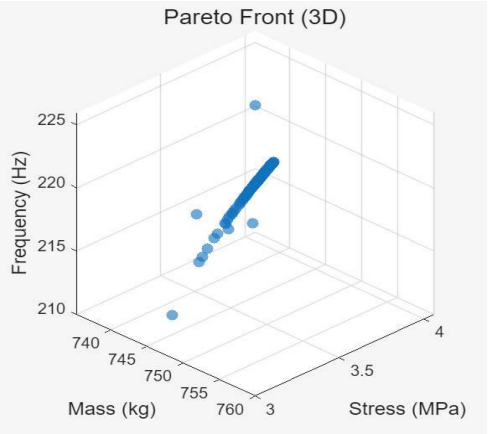

Figure 5 Pareto Result Diagram

Through optimization, a uniformly distributed Pareto optimal solution set satisfying all constraints is obtained, and representative solutions are listed in Table 4. Among them, Solution 1 is selected as the final scheme because it provides the best overall balance, with a worktable mass of 748.81 kg, a maximum coupling stress of 3.17 MPa, and a first-order natural frequency of 217.11 Hz. As shown in Table 5, the optimized design achieves significant weight reduction while largely preserving the static and dynamic performance of the system, confirming the effectiveness of IMOGWO for multi-force coupling structural optimization.

Table 4 Data Information of the Optimal Solutions

Serialnumber	x_1(mm)	x_2(mm)	x_3(mm)	Workbenchmass (kg)	Maximumcouplingstress(MPa)	Fundamentalnaturalfrequency(Hz)
1	50	75	53.86	748.81	3.17	217.11
2	50.15	75	50.49	749.66	3.17	218.13
3	50.43	75	52.23	749.16	3.17	217.59
4	50	75	48.16	750.28	3.17	218.85
5	50	75	59.96	747.22	3.17	215.24

Table 5 Parameter Comparison before and after Optimization

	Workbench mass(kg)	Maximum coupling stress(MPa)	Fundamental natural frequency(Hz)
Optimization scheme	748.81	3.17	217.11
Initial scheme	801.53	3.22	216.97
Change rate(%)	−6.58	−1.60	+0.065

Finite element validation further shows that the relative errors between the response surface predictions and simulation results remain within an acceptable engineering range. This demonstrates the high predictive accuracy of the response surface model and verifies the reliability of the optimization scheme obtained by the IMOGWO algorithm.

4 CONCLUSIONS

This study presented a multi-objective structural optimization method for a dual-drive feed system worktable under multi-force coupling conditions by integrating Response Surface Methodology and an Improved Multi-Objective Grey Wolf Optimizer. Using the depths of the end-face rectangular hole, weight-reduction cavity, and inner rectangular hole as design variables, the method minimized mass and maximum coupling stress while maximizing the first-order natural frequency. The optimized worktable reduced mass from 801.53 kg to 748.81 kg (6.58%), decreased maximum coupling stress from 3.22 MPa to 3.17 MPa (1.60%), and increased the first-order natural frequency from 216.97 Hz to 217.11 Hz (0.065%). Finite element validation confirmed the effectiveness of the proposed RSM–IMOGWO framework for lightweight and anti-vibration design of complex machine tool components.

COMPETING INTERESTS

The authors have no relevant financial or non-financial interests to disclose.

REFERENCES

[1] Seyedali Mirjalili, Shahrzad Saremi, Seyed Mohammad Mirjalili, et al. Multi-objective grey wolf optimizer: A novel algorithm for multi-criterion optimization. Expert Systems with Applications, 2016, 63: 106-119.
[2] Jesus-Maria Hernandez-Vazquez, Iker Garitaonandia, María Helena Fernandes, et al. A Consistent Procedure Using Response Surface Methodology to Identify Stiffness Properties of Connections in Machine Tools. Materials, 2018, 11(7): 1220.
[3] Li S, Hashemi Sohi S H. Lightweight Design Method for Micromanufacturing Systems Based on Multi-Objective Optimization. Micromachines, 2025, 16(9): 1032.
[4] Liu J, Liu Z T, Wu Y, et al. MBB-MOGWO: Modified Boltzmann-Based Multi-Objective Grey Wolf Optimizer. Sensors, 2024, 24(5): 1502.
[5] Ma Z C, Dong G, Liu B Q. Study on optimizing the adsorption performance of activated carbon from Rheum tanguticum stem base for methylene blue by response surface methodology. Guangdong Chemical Industry, 2025, 52(1): 14-17.
[6] Huang X, Lu Y, Shen L, et al. Solving multi-objective constrained optimization problems based on a hybrid particle swarm and grey wolf optimization algorithm. Journal of Chinese Computer Systems, 2023, 44(2): 288-299.
[7] Qi Y, Shang X J, Nie J Y, et al. Operation optimization of combined cooling, heating and power microgrid based on improved multi-objective grey wolf algorithm. Electrical Measurement & Instrumentation, 2022, 59(6): 12-19.
[8] Liu T, Zhu J J, Li J Y, et al. Energy saving optimization of gas fractionation unit based on improved MOGWO algorithm. Petroleum Processing and Petrochemicals, 2021, 52(4): 110-115.
[9] Huang J, Yuan J T, Wang Z H. Structural optimization of dual-drive feed system based on NSGA-II algorithm. China Mechanical Engineering, 2016, 27(24): 3324-3333.